

PREFERENTIAL LOW-pH DISSOLUTION OF PYROXENE IN PLAGIOCLASE-PYROXENE MIXTURES AND IMPLICATIONS FOR MARTIAN LOW-ALBEDO REGIONS. A. C. McAdam¹, M. Yu. Zolotov¹, M. V. Mironenko², and T. G. Sharp¹, ¹School of Earth & Space Exploration, Arizona State University, Tempe, AZ 85287-1404, amcadam@asu.edu, ²Vernadsky Institute of Geochemistry & Analytical Chemistry, Russian Academy of Sciences, 19 Kosygin Str., Moscow 119991, Russia.

Introduction: Mars Global Surveyor Thermal Emission Spectrometer (MGS-TES) thermal infrared (TIR) data have been used to group martian low-albedo regions into two global spectral surface types, Surface Type 1 (ST1) and Surface Type 2 (ST2). In general, TES data indicate that the plagioclase/pyroxene ratio (pl/px) is higher in ST2 (2.25-6.1) than ST1 (0.8-3.8) [1-5]. Recent study of regional spectral differences [6,7] has revealed more variation in pl/px. Also, OMEGA near-IR data indicate only weak evidence for pyroxenes in areas of the northern martian lowlands, the ST2 type locality [8]. Variations in pl/px could reflect differences in primary mineralogy [e.g., 1] and/or complications with deriving primary mineral abundances from TIR spectra caused by secondary phases [9,10]. The pl/px differences could also be caused by acid weathering. "High silica phase" (HSP) (phases difficult to distinguish in TIR spectra of Mars, such as primary volcanic glass, secondary amorphous or partially crystalline silica-rich material, clays or clay mineraloids) enrichment in the same, ST2, regions where pyroxene is comparatively depleted, is consistent with a weathering hypothesis.

Approach: We applied a kinetic dissolution model to a plagioclase-pyroxene mixture, to evaluate temporal changes in the amount of material remaining under different pH conditions and for different grain sizes. Thermodynamic equilibrium modeling was also used to explore secondary mineral formation during acid weathering of the mineral mixture.

Labradorite and augite dissolution rates for 0°C were calculated from kinetic parameters obtained by linear regression of 25 °C rate data [e.g., 11-14] using an Arrhenius equation and activation energies for labradorite (14 kcal/mol [15]) and augite (21 kcal/mol [16]) (Fig. 1). Kinetic modeling was performed under open system conditions in which solution constantly flows through the mineral grains without changing pH. This study is a continuation of [17], with the major difference being the use of augite instead of diopside. Dissolution was modeled to occur in 1 kg of grain mixture consisting of 50 vol % augite and 50 vol % labradorite. The dissolution of each mineral, presented as spherical particles, is considered separately. The model variables are initial grain diameter (0.001-10 mm) and pH (0-5). For each successive time step, mineral surface area is calculated by considering the grain size decrease from dissolution in the previous step.

To evaluate secondary mineralogy formed through dissolution of the pl-px mixture, we calculated equilib-

rium compositions in a water-mineral system open with respect to atmospheric O₂ and CO₂ at 0°C and 1 bar. To approximate the effect of px and pl dissolution rates on minerals precipitated, the amount of px or pl was increased from a 50/50 volume ratio in proportion to the difference in their rates. The H₂SO₄-HCl solution has a S/Cl molal ratio of 5.2, consistent with soil composition [18-20]. The equilibrium calculations were performed for initial solution pHs of 0-5 and water to rock (W/R) ratios of 10⁵-0.25. Trends in equilibrium secondary mineralogy with W/R can be thought of as trends with weathering progress. High W/R can represent early stages of acid weathering when pH is still low and low W/R can represent advanced weathering. This can be envisioned as titrating the solution with rock. Calculations were carried out with the GEOCHEQ code [21].

Results and Discussion: At pH values <3-4, augite dissolves faster; above this pH, labradorite dissolves faster (Fig. 1). During weathering at pH <3-4, the pl/px increases, as pyroxene preferentially dissolves (Fig. 2). The lower the solution pH (below 3-4), the faster the ratio increases. For pH values above 3-4, pl/px decreases, as plagioclase preferentially dissolves. The amount of time required to increase the pl/px in sand with 1 mm grains, from 1 (approximate lower ST1 value) to 6 (approximate upper ST2 value) is short on geologic timescales, on the order of 10²-10⁴ years, for pH 1 and 3, respectively. Smaller grain sizes result in faster weathering and faster changes in pl/px. The amount of time needed for the same increase of pl/px in a 160 μm grain mixture is ~10 years at pH 1 and ~10³ years at pH 3 (Fig. 2). The amount of time needed for a mixture of 10 μm particles, similar to martian dust (~0.2-10 μm [22]), is shorter still, <1 year at pH 1 and ~10² years at pH 3.

Note that these timescales could refer to a cumulative effect of multiple episodes of acid weathering at a constant pH. For example, these numbers may represent cumulative duration of surface alteration by acid atmospheric precipitates (rains/aerosols).

On one hand, calculated dissolution times are minimum times because experimental dissolution rates are enhanced compared to natural rates [23]. Natural rates are often slower, due to factors such as reactive grain surface area differences, pH changes, and coatings of Fe³⁺-oxides, silica, etc. On the other hand, elevated pl/px ratios observed in some low-albedo regions could reflect rapid alteration of rock surfaces. Near-IR and TIR spectral observations of martian materials access the mineralogy of a surface layer, as opposed to bulk composition.

Equilibrium calculations indicate that amorphous silica, goethite, and gypsum are produced at early stages of

weathering in systems with $\text{pHs} \leq 2$ (Fig. 3). For all systems, solutions are neutralized as weathering proceeds and W/R is decreased. As a result, the mineral assemblages formed at later stages of weathering for all systems studied have some similarities such as zeolites, clay minerals (e.g. smectites) and carbonates, though different amounts may form. Since the systems are approximately neutral when these minerals form, they will not be focused on here.

The formation of amorphous silica at lower pHs indicates a possible weathering contribution to differences in HSP abundances observed with TES. OMEGA near-IR studies of the northern plains have not found evidence of phyllosilicates [24]. However, amorphous silica is a possible constituent of HSP based on TIR spectral studies [e.g.,4,5,25]. If secondary amorphous silica is the main HSP in the northern plains, this may indicate a halting of the acid weathering early, based on our equilibrium and coupled kinetic-thermodynamic models [26,27].

For systems of an initial pH in which plagioclase dissolution dominates, goethite and kaolinite are formed early. Abundant kaolinite forms as Al is supplied to solution from plagioclase dissolution. However, the presence of kaolinite is not consistent with the lack of phyllosilicate detection in the northern plains by OMEGA [24]. It follows that amorphous silica could be a major HSP in ST2 regions, consistent with [4,5,25].

Summary: Differences in mineral dissolution rates could be, partially, responsible for variations in pl/px observed in low-albedo regions. Surfaces with high pl/px, such as several northern regions, could have experienced some preferential dissolution of pyroxenes at $\text{pHs} \sim 3-4$. Although modeled timeframes required to produce a ST2-like pl/px from an ST1-like pl/px are short on geologic timescales, they may imply multiple acid weathering events. The likely presence of amorphous silica in observations of ST2 is also consistent with weathering at $\text{pHs} \sim 3-4$.

References: [1] Bandfield J.L. et al. (2000) *Science*, 287, 1626. [2] Hamilton V.E. et al. (2001) *JGR*, 106, 14733. [3] McSween H.Y. et al. (2003) *JGR*, 108, 2003. [4] Michalski J.R. et al. (2006) *JGR*, 111, doi: 10.1029/2005JE002438. [5] Wyatt M.B. and McSween H.Y. (2002) *Nature*, 417, 263. [6] Rogers A.D. (2005) Ph.D. dissert., ASU. [7] Rogers A.D. et al. (2005) *LPS XXXVI*, Abst #2131. [8] Mustard J.F. et al. (2005) *Science*, 307, 1594. [9] Kraft M.D. et al. (2006) *LPS XXXVII*, Abst #2457. [10] Rampe E.B. et al. (2006) *Eos Trans. AGU*, 87, Abst# P21A-06. [11] Siegel D.I. and Pfannkuch H.O. (1984) *GCA*, 48, 197. [12] Sverdrup H.U. (1990) *Kinetics of Base Cation Release due to Chem. Weath.*, Lund. Univ. Press [13] Sjoberg L. (1989) *Proc. 6th Int. Symp. On Water-Rock Inter.* [14] Welch S.A. and Ullman W.J. (1993) *GCA*, 57, 2725. [15] Blum A.E. and Stillings L.L. (1995) In *Chem. Weath. Rates of Silicate Min.*, Min. Soc. Am. [16] Kump L.R. et al. (2000) *Ann. Rev. of E. and P.S.*, 28, 611. [17] McAdam A.C. et al. (2006) *LPS XXXVII*, Abst. # 2363. [18] Clark B.C. et al. (1982) *JGR*, 87, 59. [19] Foley C.N. et al. (2003) *JGR*, 108, doi: 10.1029/2002JE002019. [20] Gellert R. et al. (2006) *JGR*, 111, doi: 10.1029/2005JE002555. [21] Mironenko M.V. et al. (2000) *Herald DGGGMS RAS*, 5(15), 96. [22] Morris, R.V. et al. (2001) *JGR*, 106, 5057. [23] Brantley S.L. (2004) In *Treatise on Geochemistry*, vol. 5, 73. [24] Bibring J.P. et al. (2005) *Science*, 307, 1576. [25] Kraft M.D. et al. (2003) *GRL*, 30, doi:10.1029/2003GL018848. [26] Zolotov M.Yu. and Mironenko

M.V. (2007) *JGR*, in review. [27] Mironenko M.V. and Zolotov M.Yu. (2007), *LPS XXXVIII*, abst 1594. [28] Fergason R.L. et al. (2006) *JGR*, 111, doi:10.1029/2005JE002583.

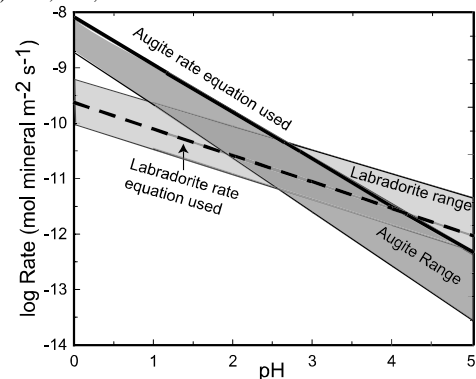


Figure 1. Mineral dissolution rates at 0°C. Ranges represent variation in experimental rates [11-14]. Lines within ranges correspond to the equation chosen for modeling.

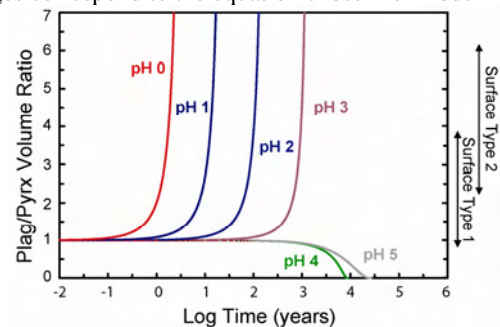


Figure 2. Change of pl/px of a 160 μm grain mixture (similar to the size of fine grains observed by MER [28]) during weathering in an open system.

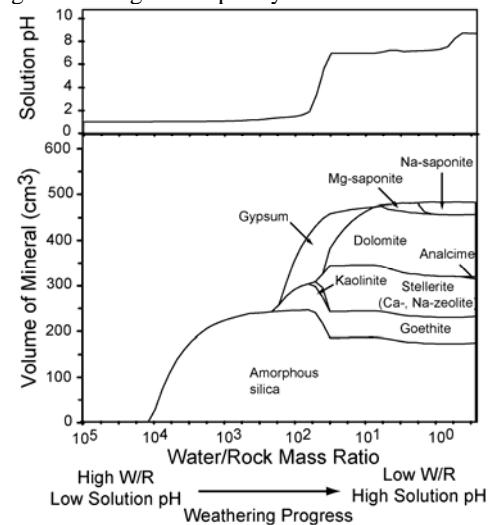


Figure 3. Equilibrium secondary minerals formed as a result of pl-px dissolution in a system with an initial solution $\text{pH}=1$. Pyroxene volume input to the system was increased from 50 vol% to 90 vol%, in proportion to its faster dissolution rate at this pH.

Acknowledgements: This work is supported by NASA MFR program grants NNG06GH14G and NNX06AB25G to M.Z. and T.S.